# On the design of a science orbit about Europa

Martin Lara* and Ryan Russell†

(as November 18, 2005)

**Abstract**

A science mission about Europa requires high-inclination low-altitude orbits. However, perturbations of Jupiter on the orbiter result in instability. Previous approaches to maximize the lifetime of the orbiter use the doubly averaged problem. We work with the unaveraged equations and find unstable periodic orbits with long lifetimes. These low-altitude repeat ground track solutions exist at all inclinations, making them suitable for mapping missions. The governing dynamics include Hill's model and a Europa gravity field based on synchronous moon theory. Inclusion of additional gravity terms is trivial to the solution method, and for the case of $J_3$, we find a marginal impact on orbit lifetime. The science orbits are found to last on the order of 1 year when the initial conditions are achieved to 11 significant digits and 4 months when only 3 siginificant digits are achieved. Finally, we demonstrate that the solutions are robust in a realistic ephemeris model, finding average lifetimes of 3 to 4 months for wide range of initial conditions with peak lifetimes of up to 6 months.

## INTRODUCTION

The instrument requirements for a scientific mission about Europa constrain the orbit design to a subset of limited values of the orbital elements. Near-circular, low-altitude, high-inclination orbits are normally required for mapping missions, and space-mission designers try to minimize the altitude variation of the satellite over the surface of the body by searching for orbits with small eccentricity and with a fixed argument of periapsis. These orbits are usually called frozen orbits [1, 2].

However, due to third body perturbations, high-inclination orbits around planetary satellites are known to be unstable [3, 4, 5], and it emerges the problem of maximizing the orbital lifetime. Dynamical systems theory is useful in orbit maintenance routines, where the stable manifold associated with unstable nominal orbits provides a nice way of maximizing time between maneuvers [6]. In the same fashion,

*Department of Ephemerides, Real Observatorio de la Armada, 11110 San Fernando, Spain

†California Institute of Technology, Jet Propulsion Laboratory, M/S 301-140L, 4800 Oak Grove Drive, CA 91109

paths in the plane of argument of periapsis and eccentricity that yield long lifetime near polar orbits around Europa have been recently identified [7].

In this paper we take a different approach. Periodic orbits around Europa are known to exist and have been previously used in the investigation of stability regions around Europa [8, 9, 10]. Periodic orbits in the rotating frame are ideal nominal repeat ground-track orbits that, for long enough repetition cycles, are suitable for mapping missions. We compute low-altitude, near-circular, highly inclined, repeat ground-track, unstable periodic orbits, and find that these kind of solutions enjoy longer lifetimes[1] than previously computed Europa science orbits. Our procedure is based on fast numeric algorithms that are easily automated. The numerical search for initial conditions of repeat ground-track orbits is very simple and feasible even for higher order gravity fields [11, 12, 13].

For our search, we use a simplified dynamical model that considers the mean gravitational field of a synchronously rotating and orbiting moon, and take into account the perturbations of the third body in the Hill problem approximation [14, 15, 4]. Tests on the validity of the solutions are made in an ephemeris model that includes perturbations of the Sun, the other Galileans, the non sphericity of Jupiter, the other gas giants, and a Europa gravity model that is consistent with synchronous moon theory and NASA's Galileo close encounters [16].

In passing from the simplified to ephemeris model we introduce a one dimensional parameter scaling of the initial conditions that proved efficient in the past [9]. On one side it provides a simple and feasible optimization for a given epoch. But it also shows how isolated is the optimized solution in the ephemeris model, thus giving a reasonable estimation of the robustness of the solution in the presence of realistic perturbing forces.

With respect to the Europa gravity field, it turns out that the Galileo flyby data cannot detect valid signatures for any gravitational terms for Europa beyond $\mu$, $J_2$, and $C_{2,2}$ [16]. Therefore, the true gravity field should be random noise centered about a synchronous theory. We calculate ideal ratios between gravitational terms for a synchronously rotating body, and a full field is based on the $J_2$ calculated from the Galilleo data. The only non-zero second degree terms are $C_{2,2} = (3/10)\, J_2$, and all terms above second degree are found to be insignificant.

Further, there is no physical reason to expect non-zero values for the $S_{n,m}$ and $C_{n,m}$ spherical harmonic terms with $n + m$ odd. Therefore, we have no reason to expect a high Europa $J_3$ value. However, based on observations of other celestial bodies and purely random chance, it seems reasonable to speculate that Europa could be top or bottom heavy [17], and previous studies have shown that $J_3$ can play an important role [17, 7, 18]. Therefore, we study the influence of $J_3$ in the proposed orbits, and find repeat ground-track orbits with higher eccentricities than the second order gravity field solutions, but with similar lifetimes.

[1] Here, "lifetime" means the time it takes the orbiter to escape Europa or impact.

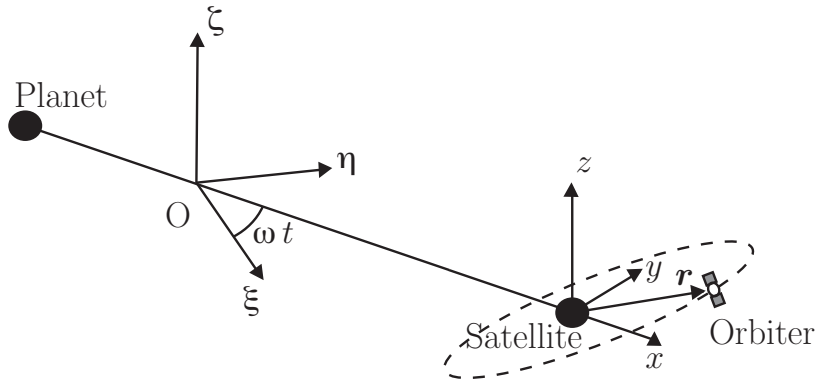


**Figure** 1: Geometry of the model showing inertial $(\xi, \eta, \zeta)$ and rotating $(x, y, z)$ frames.

## DYNAMICAL MODEL

The restricted three-body problem retains the underlying dynamics that governs the motion of an orbiter about planetary satellites (see Fig. 1). Close to the planetary satellite its physical nature in terms of a gravitational harmonics expansion must be considered. Further, the Hill problem can be used to model the planetary perturbation on a satellite's orbiter when the planet-satellite distance is sufficiently long. Then, in the rotating frame of reference with origin at the center of mass of the satellite, using Hamiltonian formulation we write

$$\mathcal{H} = (1/2)\,(\boldsymbol{X} \cdot \boldsymbol{X}) - \boldsymbol{\omega} \cdot (\boldsymbol{x} \times \boldsymbol{X}) - (\mu/r) - R(\boldsymbol{x}) \tag{1}$$

where $\boldsymbol{x} = (x, y, z)$ is the position vector of the orbiter, $r = ||\boldsymbol{x}||$, $\boldsymbol{X} = (X, Y, Z)$ is the vector of conjugated momenta —velocity in the inertial frame, $\boldsymbol{\omega}$ is the angular velocity of the satellite around the planet, $\mu$ is the satellite's gravitational parameter, and the perturbing function $R$ includes the third body and non-sphericity perturbations.

The Hamilton equations $\dot{\boldsymbol{x}} = \nabla_{\boldsymbol{X}} \mathcal{H}$, $\dot{\boldsymbol{X}} = -\nabla_{\boldsymbol{x}} \mathcal{H}$, of Eq. (1) provide

$$\ddot{\boldsymbol{x}} + 2\boldsymbol{\omega} \times \dot{\boldsymbol{x}} = -\boldsymbol{\omega} \times (\boldsymbol{\omega} \times \boldsymbol{x}) - (\mu/r^2)\,\nabla_{\boldsymbol{x}} r + \nabla_{\boldsymbol{x}} R, \tag{2}$$

equations of motion corresponding to a nonlinear dynamical system of three degrees of freedom, yet accepting the Jacobi integral $\mathcal{H}(\boldsymbol{X}, \boldsymbol{x}) = h$.

For synchronous orbiting and rotating planetary satellites, equilibrium theory expedites the representation of the satellite by a triaxial ellipsoid with matching orbital and equatorial planes, and with the axes of smaller inertia pointing to the planet. Then, the perturbing function is

$$R = (\omega^2/2)\,(3x^2 - r^2) + (\mu/r)\,N(\boldsymbol{x}). \tag{3}$$

For the non-dimensional part $N$ of the perturbing potential of the satellite, we consider

$$N = \frac{\alpha^2}{r^2}\left[J_2\left(\frac{1}{2} - \frac{3z^2}{2r^2}\right) + 3C_{2,2}\frac{x^2 - y^2}{r^2}\right] + J_3\frac{\alpha^3}{r^3}\,\frac{z}{r}\left(\frac{3}{2} - \frac{5z^2}{2r^2}\right) \tag{4}$$

where $\alpha$ is the equatorial radius of the satellite, and $J_2$, $C_{2,2}$, and $J_3$ are the harmonic coefficients with physical meaning representing oblateness, ellipticity, and pear-shapeness respectively. As we assumed equilibrium theory, we set $C_{2,2} = (3/10)\, J_2$ [19]. Despite $J_3$ is null in equilibrium theory, similarly to other celestial bodies Europa could be top or bottom heavy. Therefore, we retain $J_3$ in the simplified model to investigate the modifications that it could introduce in specific solutions.

Averaging of Eq. (1) for different perturbing functions proved very useful in studying the long term behavior around Europa [4, 20, 5, 7]. The main dynamics close to planetary satellites corresponds to the Hill problem where circular orbits suffer from instability for inclinations that depart the equatorial plane by more than $\sim 40°$ [21]. Perturbations due to the non-sphericity of the central body only introduce minor qualitative changes in the long term dynamics [14, 15, 8, 5]. However, the candidates for a Europa science orbit are among the unstable orbits. Thus, it is essential to consider the short period dynamics in the search for long lifetime orbits [7]. It seems natural, then, to proceed directly with the non-averaged problem Eqs. (1–2), where periodic orbits are the particular solutions that shall reach longest lifetimes. This is the approach we take here. Periodic orbits around Europa indeed exist in abundance, and have been previously used for a variety of dynamic applications at Europa [8, 9, 10]. Thus, proceeding as in [8, 9], we search for periodic orbits of Eq. (1) that satisfy the requisites of a science orbit about Europa.

## FAMILIES OF PERIODIC ORBITS

Periodic orbits of Hamiltonian systems appear in families. The *natural* families of periodic orbits occur for variations of the Jacobi constant, but other different families exist for variations of any of the parameters of the problem. Starting from a given periodic orbit, the whole family can be constructed with the Poincaré continuation method [22]. The initial conditions of a given periodic orbit are normally continued with differential correction algorithms that require the integration of the variational equations, and, therefore, provide the stability of the orbit as a side effect (see, for instance, [23, 24]). For the present study we have used the same predictor-corrector procedure described in [25].

The stability of periodic orbits is related to the behavior of the variational equations. For conservative systems, variations in the tangent (velocity) direction do not modify the periodic solution and, therefore, are trivial. Then, the stability character of periodic solutions to Hamiltonian systems with three degrees of freedom as Eq. (1) is obtained from two stability indices $b_1$, $b_2$, related to normal and binormal variations [26]. The condition $b_i$ real and $|b_i| < 2$ $(i = 1, 2)$ applies for linear stability, while any other possibility means instability [27]. Changes in the stability of a family can be clearly appreciated using "stability curves" [28], where the stability indices are represented as a functions of the parameter (or integral) generator of a given family.

Bifurcations of new families of periodic orbits can occur at critical values

$$b = 2\cos(2\pi\, d/n), \tag{5}$$

either for $b_1$ or $b_2$, where $d$ and $n$ are integer numbers [28] (see also [29], [30]). The bifurcation occurs from a $n$-fold periodic orbit —the $T$-periodic orbit after a period $\tau = n\,T$. We call the planar critical orbits "$d$:$n$-resonant orbits" and "$d$:$n$-resonant families" those that emerge from a $d$:$n$-resonant orbit.

In general, the variational equations are coupled. However, they uncouple for planar motions where one index, $b_1$, is related to intrinsic displacements in the normal (in-plane) direction, and the other, $b_2$, is related to perturbations in the binormal (out-of-plane) direction.

## THE RETROGRADE FAMILY

Hamiltonian Eq. (1) enjoys equatorial symmetry for $J_3 = 0$, and periodic orbits exist around the primary in the equatorial plane. Initial conditions $(x_0, 0, 0, 0, \tilde{n}\,x_0, 0)$ and period $P_0 = 2\pi/|\tilde{n}|$ in the Keplerian approximation $\tilde{n} = \pm\sqrt{\mu/x_0^3} - \omega$, are approximate enough to be improved with differential corrections until finding an exact periodic orbit of Eq. (1). Once computed a periodic orbit, the whole family can be continued for variations of the Jacobi constant.

For the values of the parameters we used the most recent available data. Thus we take $\alpha = 1565.0\,\mathrm{km}$, and $J_2 = 4.355 \times 10^{-4}$ from [31], while $\mu = 3202.7\,\mathrm{km}^3/\mathrm{s}^2$ retains the first five digits from the JUP230 solution [32], and $\omega = 2.0477 \times 10^{-5}\,\mathrm{s}^{-1}$ is the average mean motion of Europa around Jupiter in JUP230 for 200 days starting at January 1, 2025 (the epoch we used for ephemeris computations). We find it convenient to use internal units of length and time such that $\alpha = \mu = 1$. In internal units, approximate initial conditions of a grazing, equatorial, retrograde, periodic orbit are $(1, 0, 0, 0, -1.0224, 0)$, and period $T = 6.14552$.

Due to symmetries, the orbits of the family of near circular, equatorial, retrograde orbits, that we call the retrograde family, orthogonally cross the $x$ axis. Therefore, "characteristic curves" $\dot{y}_0 = \dot{y}_0(x_0)$ can be used to represent the family [28]. Figure 2 presents the retrograde family in the vicinity of Europa ($\alpha < r < 2\alpha$). The stability diagram in the right plot of Fig. 2 shows that equatorial, retrograde, near circular, periodic orbits are always stable.

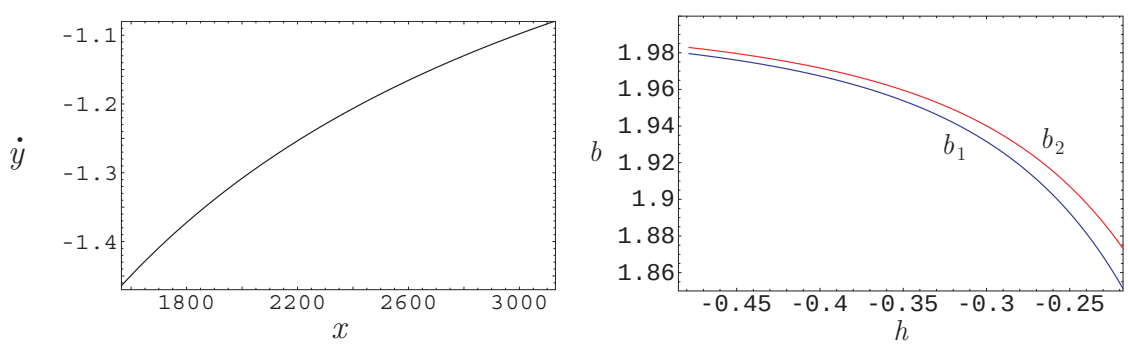


**Figure** 2: The retrograde family close to Europa. Left: characteristic curve $\dot{y}_0 = \dot{y}_0(x_0)$; units are km and km/s. Right: stability diagram; $h$ is in internal units.

## FAMILIES OF 3-D PERIODIC ORBITS CLOSE TO EUROPA

For a given $d$:$n$ resonance, we compute $b_2$ from Eq. (5). Then, we search the retrograde family until finding the orbit corresponding to the computed $b_2$ value. This orbit will be $d$:$n$-resonant —the spacecraft orbits Europa $n$ times while Europa orbits Jupiter $d$ times— producing the bifurcation of a new family of three-dimensional periodic orbits that repeat themselves after $(n-d)$ upward crossings of the equatorial plane, or cycles[2]. Thus, for instance, $b_2 \approx 1.97656$ corresponds to the 1:41-resonant orbit. Different types of vertical bifurcations can exist [33], and the vertically bifurcated families are easily computed.

We assume inclination limits $70° < i < 110°$ for the scientific mission, and assume also that it requires an altitude close to one hundred km over the surface of Europa. Therefore, we limit ourselves to computing the 1:42-, 2:83-, and 1:41-resonant families, which, as Fig. 3 shows, can satisfy these requirements. Higher order resonances will provide many other orbits satisfying those requisites.

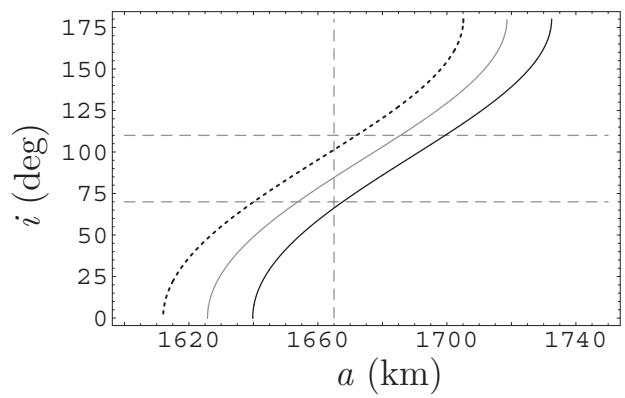


**Figure** 3: Averaged semi-major axis versus averaged inclination for the 1:42- (dotted), 2:83- (gray), and 1:41- (black) resonant families.

Figure 4 presents the stability diagrams of these three families in terms of the Jacobi constant and averaged inclination. The three families are made of low-eccentricity orbits with unstable character in the range of inclinations $49° < i < 133.5°$. Note that, in every case, $b_1$ remains with almost constant value inside the interval $75° < i < 105°$. The higher $b_1$ values of the 2:83-resonant family are associated to the the fact that the orbits of this family have much longer period than the orbits of the other families. In what follows, we only present results for orbits of the 1:41-resonant family. Experiments performed with orbits of the other families produced very similar results.

Figure 5 shows a sample orbit of the 1:41-resonant family with averaged orbital elements $a = 1683.217$ km, $e = 0.0009$, $i = 90.001°$. The evolution of the instantaneous orbital elements in one period is also presented, where two kinds of short period effects are observed. One produces fast oscillations of the orbital elements with half

[2]Note that orbits pertaining to a $d$:$n$-resonant family are not resonant orbits except for the bifurcation orbit.

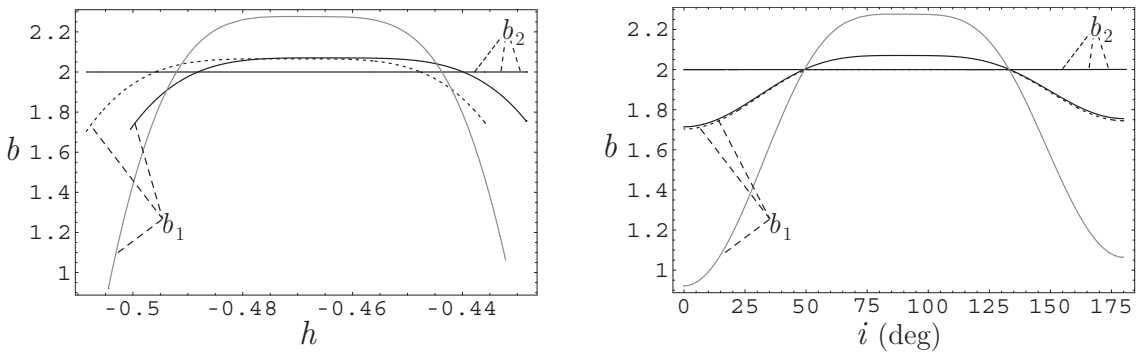


**Figure** 4: Stability diagrams of the 1:42- (dotted), 2:83- (gray), and 1:41- (black) resonant families. Left: Jacobi constant $h$. Right: averaged inclination $i$.

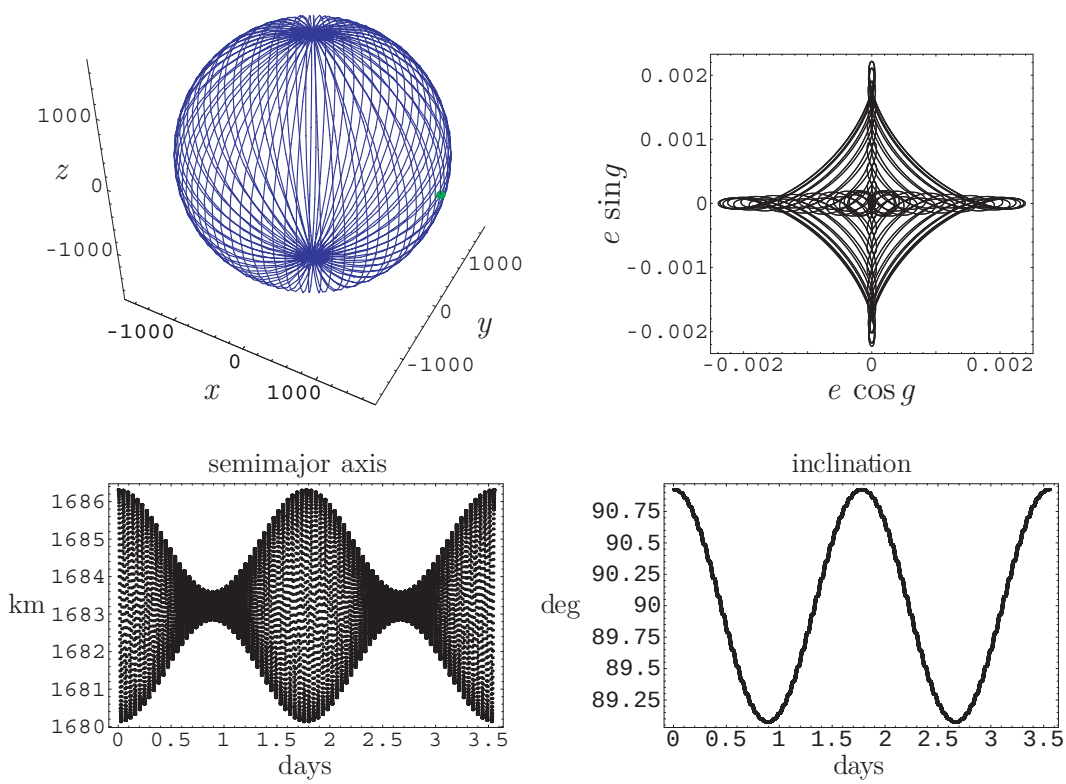


**Figure** 5: Sample repeat ground-track orbit after 40 cycles, and one period evolution of the instantaneous orbital elements.

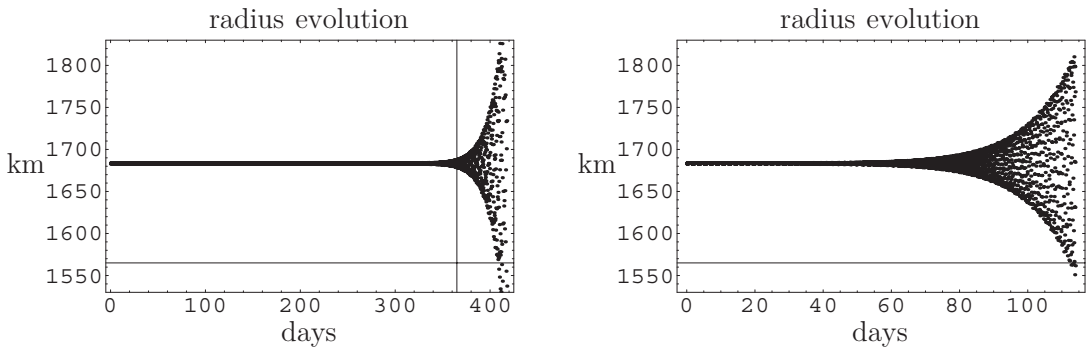


**Figure** 6: Long term propagation of the unstable, polar periodic orbit after 40 cycles. The horizontal axis marks the surface of Europa. Left: $\epsilon < 10^{-11}$. Right: $\epsilon < 10^{-3}$.

the period between two consecutive upward crossings of the equatorial plane of the periodic orbit; these oscillations scarcely affect the instantaneous inclination. These small amplitude, very short period oscillations are modulated by an oscillation with half the frequency of the periodic orbit, the smaller amplitudes corresponding to the times where the orbital plane is perpendicular to the $x$-$z$ plane.

Note that the periodic orbits are periodic only within certain numerical precision $\epsilon = \max|\xi_i(T) - \xi_i(0)|$ $(i = 1, \ldots, 6)$, where $\xi_i$ stands for any of the coordinates in phase space. The periodicity error $\epsilon$ together with rounding errors play the role of small perturbations in a long term propagation, where the orbiter enters the unstable manifold of the unstable periodic orbit. Then, the exponential increase of the eccentricity forces the orbiter to impact Europa. Figure 6 shows two sample propagations for the polar orbit above. In the left plot the orbit remains periodic for almost one year and delays the impact to Europa to more than 400 days. We started from a periodic orbit with periodicity $\epsilon < 10^{-11}$ in internal units, that amounts to better than one millimeter in position and $10^{-4}$ mm/s in velocity, that is highly unrealistic from a practical point of view. The periodicity of the starting orbit used in the right plot is of the order of 1 km in position and 1 m/s in velocity, and the lifetime reduces to about 110 days.

The lifetime of the orbiter can be enlarged by taking initial conditions from the stable manifold of the periodic orbit. A detailed study is in progress and results will be presented elsewhere.

## VARIATIONS OF $J_3$

To investigate how the possible non uniform density of Europa affects the behavior of the Europa science orbit, now we consider a pear-shaped Europa. We compute families of periodic orbits for variations of $J_3$ starting from the solutions above, and assuming a limit value $|J_3| = C_{2,2}$. Figure 7 shows the stability diagram of the family of polar periodic orbits after 40 cycles, for variations of $J_3$. The index $b_2$ is always very close to $b_2 = 2$ and is not presented. From Fig. 7 we conclude that $J_3$ does not worsen the stability behavior, in fact it sligthly improves. This is expected because

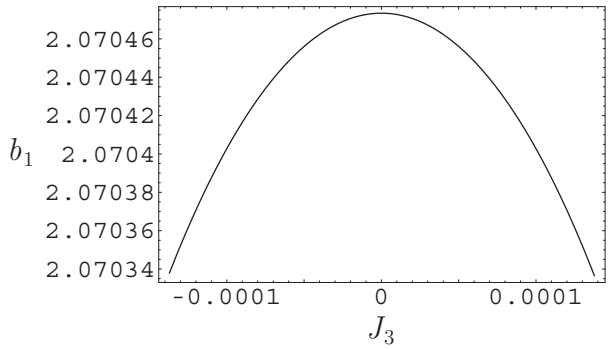


**Figure** 7: Family of polar, periodic orbits after 40 cycles for variations of $J_3$: $b_1$ stability curve.

the primary origin of the dynamical instability of high inclination orbits is the third body perturbation on the central body attraction.

Figure 8 shows one period evolution of the instantaneous orbital elements of a polar orbit of the 1:41-resonant family with $J_3 = 1.3784 \times 10^{-4}$, and averaged orbital elements $a = 1683.224$ km, $e = 0.02478$, $i = 89.9972°$, $g = 270°$. As $J_3$ breaks the equatorial symmetry, low eccentricity periodic orbits no longer exist [2]. In agreement to [7], we note that negative $J_3$ values will produce low eccentricity orbits with $g = 90°$ whereas positive $J_3$ values produce low eccentricity orbits with $g = 270°$. Except for having a higher value of the eccentricity, the instantaneous orbital elements behave very similar to the $J_3 = 0$ case, with the higher oscillations corresponding to instantaneous retrograde inclinations.

Since the stability indices remain almost identical to the $J_3 = 0$ case, we should expect similar behavior in long term integrations. Compared to the $J_3 = 0$ case, we might expect faster accumulation of rounding errors due to the higher values of the eccentricity —that we did not appreciate in our experiments. Figure 9 shows similar examples to the case $J_3 = 0$, where similar lifetimes are reached.

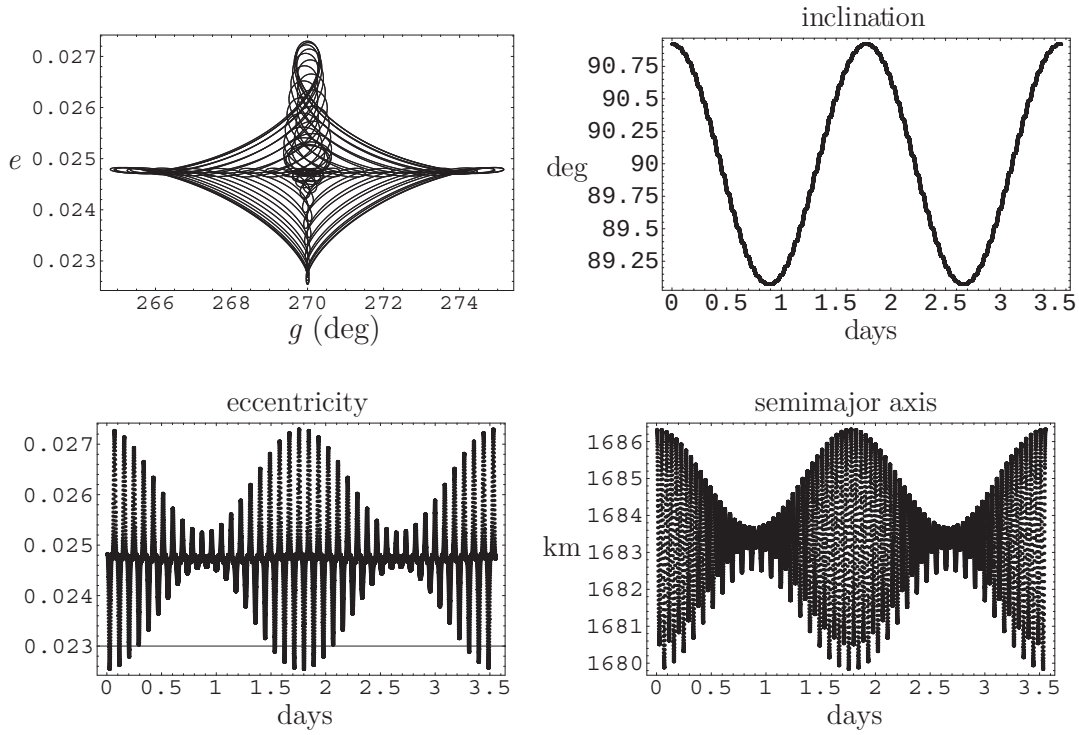


**Figure** 8: One period evolution of the instantaneous orbital elements for a polar orbit periodic after 40 cycles ($J_3 \sim C_{2,2}$).

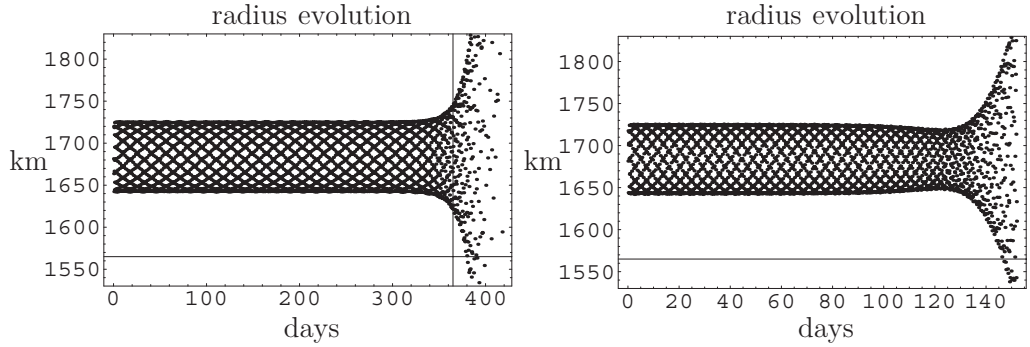


**Figure** 9: Long term propagation of a polar periodic orbit after 40 cycles ($J_3 \sim C_{2,2}$). The horizontal axis marks the surface of Europa. Left: $\epsilon < 10^{-11}$. Right: $\epsilon < 10^{-3}$.

## EPHEMERIS MODEL

The ephemeris model is based on three publicly available estimated solutions for the parameters, positions, velocities, and orientations of celestial bodies of interest (see [34]). Namely, the JUP230 solution [32], based on Galileo data, for the parameters and body states associated with the Jupiter system. The DE405 solution [35, 36] for each of the major planets. And the `pck00008.tpc` file [37], primarily based on the results from the IAU/IAG Working Group on Cartographic Coordinates and Rotational Elements of the Planets and Satellites in 2000 [38], for the body orientation information. The specific bodies and associated parameters used for all ephemeris propagations in this study are included in Tables 1 and 2.

| Body | $GM$ (km$^3$/s$^2$) | $GM$ source | Position source |
|---|---|---|---|
| Io | 5.959916033410404E+03 | JUP230 | JUP230 |
| Europa | 3.202738774922892E+03 | JUP230 | JUP230 |
| Ganymede | 9.887834453334144E+03 | JUP230 | JUP230 |
| Callisto | 7.179289361397270E+03 | JUP230 | JUP230 |
| Jupiter | 1.266865349218008E+08 | JUP230 | JUP230 |
| Saturn | 3.794062976400000E+07 | JUP230 | DE405 |
| Uranus | 5.794548600000000E+06 | JUP230 | DE405 |
| Neptune | 6.836534900000000E+06 | JUP230 | DE405 |
| Sun | 1.327132332402215E+11 | JUP230 | DE405 |

**Table** 1: Active bodies and gravitational parameters

| Body | Term | Un-normalized value | Source |
|---|---|---|---|
| Europa | $J_2$ | 4.355E−04 | Ref. [31] |
| Europa | $C_{2,2}$ | $(3/10)\,J_2$ | Sync. moon theory |
| Jupiter | $J_2$ | 1.469642900697847E−02 | JUP230 |
| Jupiter | $J_3$ | −6.436411055625769E−07 | JUP230 |
| Jupiter | $J_4$ | −5.871402915754995E−04 | JUP230 |
| Jupiter | $J_6$ | 3.425025517100406E−05 | JUP230 |

**Table** 2: Non-zero spherical harmonic coefficients for the active bodies

For a given epoch, the inertial directions of the instantaneous Jupiter-Europa vector $\boldsymbol{\rho} = \boldsymbol{r}_E - \boldsymbol{r}_J$ and the system angular momentum $\boldsymbol{h} = \boldsymbol{\rho} \times (\boldsymbol{v}_E - \boldsymbol{v}_J)$ are used to define a coordinate rotation to the ephemeris system. Vectors $\boldsymbol{r}$ and $\boldsymbol{v}$ are position and velocity in the ephemeris system, while subscripts $E$ and $J$ stand for Europa and Jupiter respectively. Thus, the mapping $\mathcal{F} : (\boldsymbol{x}, \dot{\boldsymbol{x}}) \longrightarrow (\boldsymbol{r}, \boldsymbol{v})$ from the rotating, Europa centered frame to the inertial frame with origin at the baricenter of the Jupiter system is

$$\boldsymbol{r} = \boldsymbol{r}_E + \boldsymbol{R}\,\boldsymbol{x}, \qquad \boldsymbol{v} = \boldsymbol{v}_E + \dot{\boldsymbol{R}}\,\boldsymbol{x} + \boldsymbol{R}\,\dot{\boldsymbol{x}} \tag{6}$$

where the elements of the rotation matrix $\boldsymbol{R} = (\boldsymbol{u}_x, \boldsymbol{u}_y, \boldsymbol{u}_z)$ are

$$\boldsymbol{u}_x = \boldsymbol{\rho}/||\boldsymbol{\rho}||, \qquad \boldsymbol{u}_z = \boldsymbol{h}/||\boldsymbol{h}||, \qquad \boldsymbol{u}_y = \boldsymbol{u}_z \times \boldsymbol{u}_x$$

Once we passed from the simplified model to the true (ephemeris), long term propagations of the initial conditions will provide the real lifetimes of the selected orbits. Note, however, that the ephemeris runs are attached to a given epoch, and so are the conclusions regarding lifetimes. To test the general validity of the lifetimes we could make a variety of runs for different epochs. We prefer to proceed distinctly: we perform all the ephemeris runs for a fixed epoch (January 1, 2025) and use a one dimensional scaling parameter $k$ that proved very useful in the past [9].

The $k$-scaling in the range $0.97 < k < 1.03$ accounts for variations in the distance from Europa to Jupiter —on the order of a few percent of its nominal value— produced by the non-zero eccentricity of the orbit of Europa and slight perturbations in semi-major axis. Then, after the transformation from Eq. (6), we scale the initial state to

$$\boldsymbol{x}' = k\,\boldsymbol{x}, \qquad \dot{\boldsymbol{x}}' = \dot{\boldsymbol{x}}\,\sqrt{1/k}, \tag{7}$$

where the nonlinear scaling of the velocity results from assumming Europa maintains its circular velocity although the Jupiter-Europa distance is slightly scaled. Consequently, assumed it remains periodic, the period of the scaled spacecraft orbit should be $T' = T\,\sqrt{k^3}$. After each scaling for a given $k$ we perform the propagation and plot the resulting lifetime $\tau$.

Figure 10 presents results for the $J_3 = 0$ case corresponding the 40 cycle periodic orbit for different inclinations. Lifetimes $\tau$ average to about four months with peaks of more than six months, where the best results side with the polar orbits. The plot at the top corresponds to the $k$-scaling of initial conditions $(x, 0, 0, 0, \dot{y}, \dot{z})$, while at the bottom the initial conditions are close to the $y$ axis. Table 3 provides initial conditions of the several periodic orbits in the simplified model.

| $i$ (deg) | $x$ (km) | $\dot{y}$ (km/s) | $\dot{z}$ (km/s) | Period (days) |
|---|---|---|---|---|
| 100 | 1690.689890962806 | −0.2954850833646089 | −1.352955033637386 | 3.576074029604334 |
| 90 | 1682.559086494749 | −0.5671495124122091 | −1.381021094488744 | 3.550476907604339 |
| 80 | 1674.566451069315 | 0.1845444542009359 | −1.367096125801892 | 3.525113167610515 |

**Table** 3: Initial conditions of several 40-cycle periodic orbits ($y = z = \dot{x} = 0$, $J_3 = 0$)

The case $k = 1$ typically results in repeat ground-track orbits of the ephemeris model, where the ground trace doest not drift substantially from its nominal value. However, the lifetime optimization provided by the $k$-scaling normally destroys the repeat ground trace condition (see Fig. 11). This lack of repeating ground tracks may in fact be preferred from a mapping perspective because it provides a more complete global surface coverage.

Figure 12 shows similar results for the $J_3 \sim C_{2,2}$ case, where we note that the lifetimes are not significantly affected.

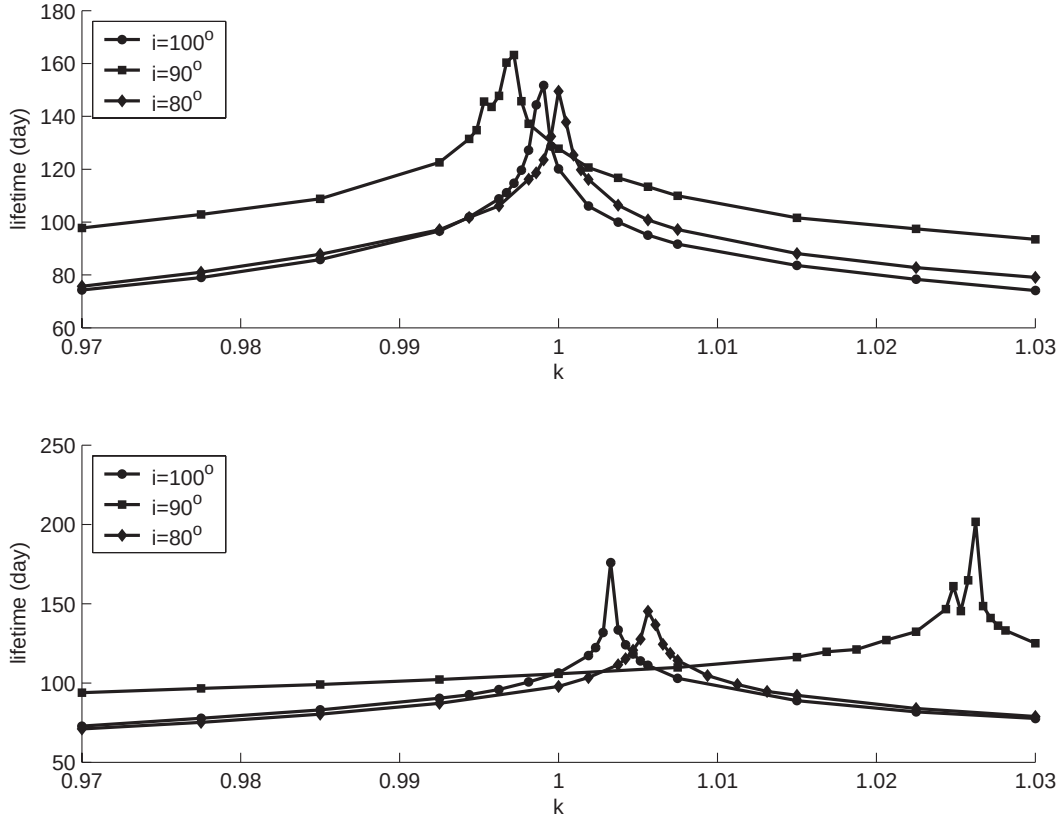


**Figure** 10: Ephemeris runs corresponding to periodic orbits after 40 cycles in the simplified model ($J_3 = 0$). Initial conditions on the $x$ axis (top), and close to the $y$ axis (bottom).

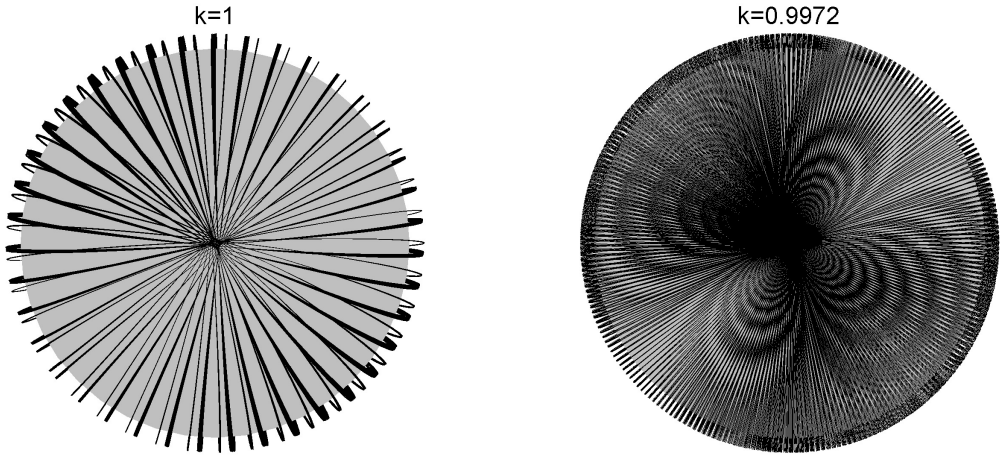


**Figure** 11: Three month propagations in the ephemeris model ($i = 90°$, $J_3 = 0$, initial conditions on the $x$ axis). Left: repeat ground-track orbit after 40 cycles with a lifetime of 128 days. Right: lifetime of 163 days without repetition of the ground track.

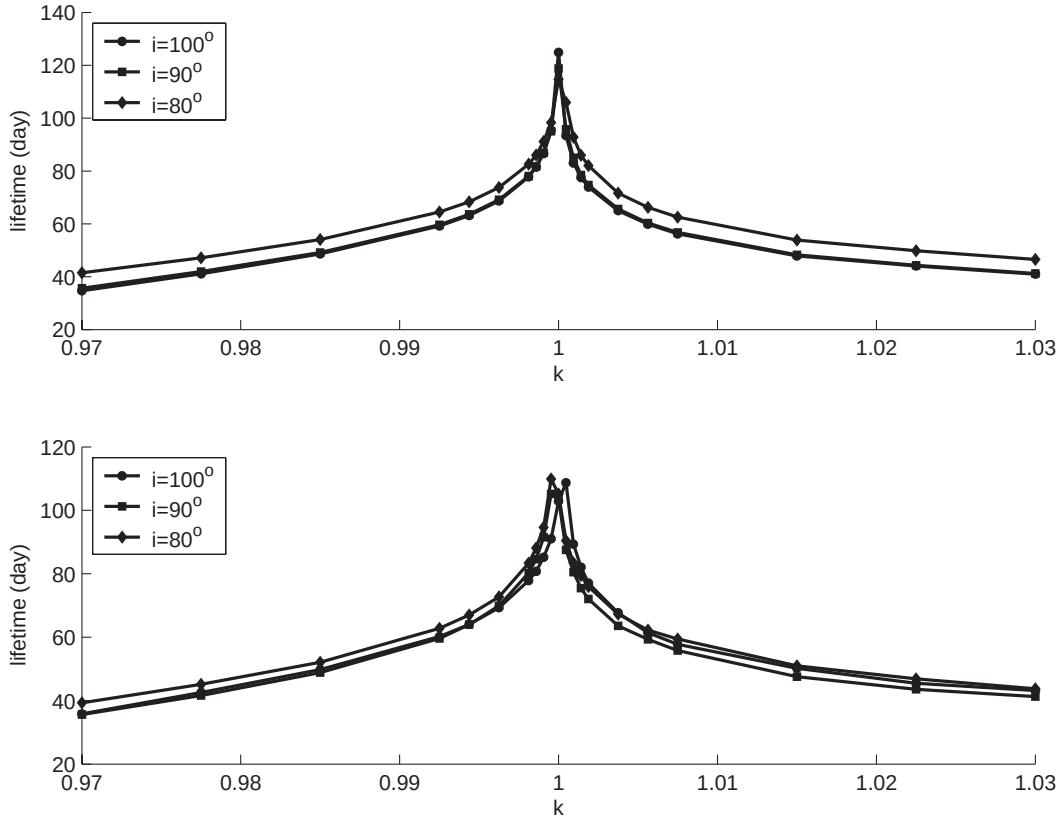


**Figure** 12: Ephemeris runs for $J_3 \sim C_{2,2}$. Initial conditions close to the $x$ axis (top), and the $y$ axis (bottom).

Note that the curve $\tau = \tau(k)$ provides a reasonable estimation of the robustness of the solution, i.e., how sensitive is it to initial conditions in the ephemeris model. Further, the one dimensional $k$-scaling can be seen as a feasible optimization of the initial state —that allowed us to find orbits with lifetimes of six months in the ephemeris model. We must emphasize that the $k$-scaling does not optimize a random choice of initial conditions for a science orbit, that typically produce orbits with lifetimes shorter than one month.

Because the ephemeris model contains many perturbations that are unaccounted for in our simple model, we find it difficult to predict what values of $k$ will lead to the longest lifetime orbits. However, by picking an epoch and performing an educated one-dimensional search, we present a simple method for demonstrating and finding long lifetime ephemeris solutions with the underlying assumption that the ephemeris force model is known. Although, we believe the force model considered in this study will capture the first order dynamics of a close orbiter around Europa, the remaining challenge is to consider the effect of the higher order terms, such as the full gravity field at Europa, that are certainly non-zero but will remain unknown until after a

science orbit is achieved.

## CONCLUSIONS

The computation of periodic solutions of a Hill perturbed problem reveals as a versatile and fast procedure for searching for long lifetime repeat ground-track orbits around Europa. Close to Europa, the repetition cycle is long enough to satisfy the requirements of a science orbit.

The simplified model retains the underlaying dynamics governing the motion close to Europa. Notably, we have found science orbits lasting more than six months in the ephemeris model. Further, our solutions are quite robust, and the lifetimes average to about four months in a wide region around the optimum set of initial conditions. These lifetimes are consistent with previous ephemeris studies. A detailed study of the stable-unstable manifolds associated to the periodic solutions of this paper is in progress, and it could provide initial conditions for science orbits even with longer lifetimes. However, because of radiation it is questionable that the spacecraft will survive more than six months around Europa.

We only consider a second order gravity field although perturbations from other harmonics will probably exist. However, the instability that affects high inclination orbits has its dynamic origin in the third-body perturbation. Therefore, perturbation from gravitational harmonics of order higher than two should only affect the shape of the orbit, producing negligible effects on stability. Experiments with different values of $J_3$ support this hypothesis.

The one dimensional scaling we used in the ephemeris model might also be useful answering two questions that have not been addressed in previous analytic studies. Namely, given analytic derived initial conditions in a simpler dynamical model, how long can we expect the same orbit to last in a true ephemeris. And how isolated is the longest lifetime orbit, or how large is the radius of the long-lifetime phase space. Both of these are very practical questions that the anticipated Europa Orbiter project will certainly ask.

### ACKNOWLEDGEMENTS

Part of this work has been performed at the Jet Propulsion Laboratory, California Institute of Technology, under a contract with the National Aeronautics and Space Administration. Martin Lara acknowledges partial support from the Spanish Government (project numbers ESP2004-04376 and ESP-2005-07107).

# References


[1] Cutting, E., Born, G.H., and Frautnick, J.C., "Orbit Analysis for SEASAT-A," *The Journal of the Astronautical Sciences,* Vol. 26, 1978, pp. 315–342.

[2] Coffey, S., Deprit, A., and Deprit, E., "Frozen Orbits for Satellites Close to an Earth-like Planet," *Celestial Mechanics and Dynamical Astronomy,* Vol. 59, 1994, pp. 37–72.

[3] Johannesen, J.R., and D'Amario, L.A., "Europa Orbiter Mission Trajectory Design," paper AAS 99–360, presented at the 1999 AAS/AIAA Astrodynamics Specialist Conference, Girdwood, Alaska, August 1999.

[4] Scheeres, D.J., Guman, M.D., and Villac, B.F., "Stability Analysis of Planetary Satellite Orbiters: Application to the Europa Orbiter," *Journal of Guidance, Control, and Dynamics*, Vol. 24, No. 4, 2001, pp. 778–787.

[5] Lara, M., San-Juan, J.F., and Ferrer, S., "Secular Motion around TriAxial, Synchronously Orbiting, Planetary Satellites: Application to Europa," *Chaos: An Interdisciplinary Journal of Nonlinear Science*, Vol. 15, No. 4, 2005, pp. 1–13.

[6] Gomez, G., Llibre, J., Martinez, R., and Simó, C., *Dynamics and Mission Design Near Libration Points. Vol. I Fundamentals: The Case of Collinear Libration Points*, World Scientific Monograph Series in Mathematics, Vol. 2, World Scientific, Singapore–New Jersey–London–Hong Kong, 2001.

[7] Paskowitz, M.E., and Scheeres, D.J., "Transient Behavior of Planetary Satellites Including Higher Order Gravity Fields," paper AAS 2005-358, presented at the 2005 Astrodynamics Specialists Conference, Lake Tahoe, California, August 2005.

[8] Lara, M., and San-Juan, J.F., "Dynamic Behavior of an Orbiter Around Europa," *Journal of Guidance, Control and Dynamics*, Vol. 28, No. 2, 2005, pp. 291–297.

[9] Lara, M., Russell, R., and Villac, B., "On Parking Solutions Around Europa" paper AAS 2005-384, presented at the 2005 AAS/AIAA Astrodynamics Specialist Conference, Lake Tahoe, California, August 2005.

[10] Russell, R., "Global Search for Planar and Three-dimensional Periodic Orbits Near Europa," paper AAS 2005-290, presented at the 2005 AAS/AIAA Astrodynamics Specialist Conference, Lake Tahoe, California, August 2005.

[11] Lara, M., *SADSaM: A Software Assistant for Designing SAtellite Missions*, CNES report no. DTS/MPI/MS/MN/99-053, May 1999, 75 pp.

[12] Lara, M., "Searching for Repeating Ground Track Orbits: A Systematic Approach," *The Journal of the Astronautical Sciences*, Vol. 47, 1999, pp. 177–188.

[13] Lara, M., "Repeat Ground Track Orbits of the Earth Tesseral Problem as Bifurcations of the Equatorial Family of Periodic Orbits," *Celestial Mechanics and Dynamical Astronomy*, Vol. 86, No. 2, 2003, 143–162.

[14] Kozai, Y., "Motion of a Lunar Orbiter," *Publications of the Astronomical Society of Japan*, Vol. 15, No. 3, 1963, pp. 301–312.

[15] Lidov, M. L., and Yarskaya, M. V., "Integrable cases in the problem of the evolution of a satellite orbit under the joint effect of an outside body and of the noncentrality of the planetary field," *Kosmicheskie Issledovaniya*, Vol. 12, Mar.-Apr. 1974, pp. 155–170.

[16] Anderson, J.D., Schubert, G., Jacobson, R.A., Lau, E.L., Moore, W.B., and Sjogren, W.L., "Europa's differentiated internal structure: Inferences from four Galileo encounters," *Science*, Vol. 281, 1998, pp. 2019–2022.

[17] Aiello, J., "Numerical Investigation of Mapping Orbits about Jupiter's Icy Moons," paper AAS 2005-377, presented at the 2005 Astrodynamics Specialists Conference, Lake Tahoe, California, August 2005.

[18] Paskowitz, M.E., and Scheeres, D.J., "Orbit Mechanics About Planetary Satellites Including Higher Order Gravity Fields," paper AAS 2005-190, presented at the 2005 Space Flight Mechanics Meeting, Copper Mountain, Colorado, January 2005.

[19] Bursa, M., "Figure and Dynamic Parameters of Synchronously Orbiting Satellites in the Solar System," *Bulletin of the Astronomical Institute of Czechoslovakia,* Vol. 40, No. 2, 1989, pp. 125–130.

[20] Paskowitz, M.E. and Scheeres, D.J., "Orbit Mechanics about Planetary Satellites," paper AAS 04-244, presented at the Space Flight Mechanics Meeting, Maui, Hawaii, February 2004.

[21] Broucke, R., "Long-Term Third-Body Effects via Double Averaging,", *Journal of Guidance, Control and Dynamics*, Vol. 26, No. 1, 2003, pp. 27–32.

[22] Siegel, and C., Moser, J.K., *Lectures on Celestial Mechanics*, Springer-Verlag, Berlin, 1971.

[23] Simó, C., "On the Analytical and Numerical Approximation of Invariant Manifolds," *Modern Methods in Celestial Mechanics, Comptes Rendus de la 13ieme Ecole Printemps d'Astrophysique de Goutelas (France), 24-29 Avril, 1989*, D. Benest and C. Froeschle (eds.), Editions Frontieres, Paris, 1990, pp. 285–389.

[24] Deprit, A., and Henrard, J., "Natural families of periodic orbits," *Astronomical Journal*, Vol. 72, No. 2, 1967, pp. 158–172.

[25] Lara, M., and Peláez, J., "On the Numerical Continuation of Periodic Orbits: An Intrinsic, 3-Dimensional, Differential, Predictor-Corrector Algorithm," *Astronomy and Astrophysics*, Vol. 389, February 2002, pp 692–701.

[26] Deprit, A., "Intrinsic variational equations in three dimensions," *Celestial Mechanics*, Vol. 24, 1981, pp. 185–193.

[27] Broucke, R., "Stability of Periodic Orbits in the Elliptic Restricted Three-Body Problem," *AIAA Journal*, Vol. 7, No. 6, 1969, pp. 1003–1009.

[28] Hénon, M., "Exploration Numérique du Problème Restreint. II. Masses égales, stabilité des orbites périodiques," *Ann. and Astrophys.*, Vol. 28, No. 2, 1965, pp. 992–1007.

[29] Robin, I.A., and Markellos, V.V., "Numerical Determination of Three-dimensional Periodic Orbits Generated from Vertical Self-resonant Orbits," *Celestial Mechanics*, Vol. 21, 1980, pp. 395–434.

[30] Davoust, E., and Broucke, R., "A Manifold of Periodic Orbits in the Planar General Three-body Problem with Equal Masses," *Astronomy and Astrophysics,* Vol. 112, 1982, pp. 305–320.

[31] *Jupiter, The Planet, Satellites, and Magnetosphere*, F. Bagenal, T. Dowling, W. McKinnon (eds.), Cambridge Planetary Society, Cambridge, United Kingdom, 2004, p. 285.

[32] URL: `ftp://naif.jpl.nasa.gov/pub/naif/generic_kernels/spk/satellites/jup230.bsp` [cited 22 June 2005].

[33] Hénon, M., "Vertical Stability of Periodic Orbits in the Restricted Problem. I. Equal masses", *Astronomy and Astrophysics*, Vol. 28, 1973, pp. 415–426.

[34] URL: `http://naif.jpl.nasa.gov/naif/spiceconcept.html` [cited 22 June 2005].

[35] URL: `ftp://naif.jpl.nasa.gov/pub/naif/generic_kernels/spk/planets/de405_2000-2050.bsp` [cited 22 June 2005].

[36] Standish, E. M., *JPL Planetary and Lunar Ephemerides*, CD-ROM, Willman-Bell Inc., Richmond, VA, 1997.

[37] URL: `ftp://naif.jpl.nasa.gov/pub/naif/generic_kernels/pck/pck00008.tpc` [cited 22 June 2005].

[38] Seidelmann, P.K., Abalakin, V.K., Bursa, M., Davies, M.E., Bergh, C. de, Lieske, J.H., Oberst, J., Simon, J.L., Standish, E.M., Stooke, P., and Thomas, P.C., "Report of the IAU/IAG Working Group on Cartographic Coordinates and Rotational Elements of the Planets and Satellites: 2000," *Celestial Mechanics and Dynamical Astronomy*, Vol. 82, No. 1, 2002, pp. 83–111.